

1 **Record-low Arctic stratospheric ozone in 2020: MLS**
2 **observations of chemical processes and comparisons**
3 **with previous extreme winters**

4 **Gloria L Manney^{1,2}, Nathaniel J Livesey³, Michelle L Santee³, Lucien**
5 **Froidevaux³, Alyn Lambert³, Zachary D Lawrence^{4,1}, Luis F Millán³, Jessica L**
6 **Neu³, William G Read³, Michael J Schwartz³, Ryan A Fuller³**

7 ¹NorthWest Research Associates, Socorro, NM, USA

8 ²New Mexico Institute of Mining and technology, Socorro, NM, USA

9 ³Jet Propulsion Laboratory, California Institute of Technology, Pasadena, CA, USA

10 ⁴National Oceanic and Atmospheric Administration / Cooperative Institute for Research in

11 Environmental Sciences, Boulder, CO, USA

12 **Key Points:**

- 13 • MLS trace gas data show that exceptional polar vortex conditions led to record-
- 14 low ozone in the Arctic lower stratosphere in 2019/2020
- 15 • Early and persistent cold conditions led to the longest period with chlorine in ozone-
- 16 destroying forms in the 16-year MLS data record
- 17 • Chemical ozone destruction began earlier than in any Arctic winter in the MLS
- 18 record and ended later than in any year except 2010/2011

Abstract

Aura Microwave Limb Sounder (MLS) measurements show that chemical processing was critical to the observed record-low Arctic stratospheric ozone in spring 2020. The 16-year MLS record indicates more polar denitrification and dehydration in 2019/2020 than in any Arctic winter except 2015/2016. Chlorine activation and ozone depletion began earlier than in any previously observed winter, with evidence of chemical ozone loss starting in November. Active chlorine then persisted as late into spring as it did in 2011. Empirical estimates suggest maximum chemical ozone losses near 2.8 ppmv by late March in both 2011 and 2020. However, peak chlorine activation, and thus peak ozone loss, occurred at lower altitudes in 2020 than in 2011, leading to the lowest Arctic ozone values ever observed at potential temperature levels from ~ 400 –480 K, with similar ozone values to those in 2011 at higher levels.

Plain Language Summary

Unlike the Antarctic, the Arctic does not usually experience an ozone hole because temperatures are often too high for the chemistry that destroys ozone. In 2019/2020, satellite measurements show record-low stratospheric wintertime temperatures and record-low springtime ozone concentrations in the Arctic lower stratosphere (about 12–20 km altitude). Only one other winter/spring season, 2010/2011, in this 16-year satellite data record comes close. Low temperatures, which result in chlorine being converted from non-reactive forms into forms that destroy ozone, started earlier than in any previous Arctic winter in the record and lingered later than in any year except 2011. The ozone-destroying chemistry in 2019/2020 occurred at lower altitudes (where more of the ozone that filters out harmful ultraviolet radiation resides) than in 2010/2011. Such extensive ozone loss can have important health and biological impacts because it leads to more ultraviolet radiation reaching the Earth's surface. While the success of the Montreal Protocol in limiting human emissions that increase ozone-destroying gases in the stratosphere has resulted in much less Arctic ozone destruction than we would have otherwise had, future temperature changes could lead to other winters with even more chemical ozone depletion than in 2019/2020.

1 Introduction

Arctic chemical ozone loss varies dramatically because of extreme interannual variations in the meteorology of the stratospheric polar vortex (e.g. WMO, 2018). For the past 16 years, the Aura Microwave Limb Sounder (MLS) has provided a uniquely comprehensive suite of daily global measurements for studying lower stratospheric polar chemical processing. The two previous Arctic winters on record with coldest conditions and greatest ozone loss occurred during this period: In 2010/2011, although lower stratospheric minimum temperatures did not consistently set records, exceptionally prolonged (lasting into April) cold led to unprecedented Arctic chemical ozone loss (e.g., Manney et al., 2011; Sinnhuber et al., 2011; Kuttippurath et al., 2012; WMO, 2014). December 2015–January 2016 Arctic temperatures were the lowest in at least 68 years (Manney & Lawrence, 2016; Matthias et al., 2016), Arctic denitrification and dehydration were the most severe in the MLS record (e.g., Manney & Lawrence, 2016; Khosrawi et al., 2017), and ozone dropped more rapidly than in 2010/2011. Cumulative ozone loss did not match or surpass that in 2011 only because a major final warming in early March 2016 halted chemical processing and dispersed processed air from the vortex (Manney & Lawrence, 2016; Johansson et al., 2019). In 2019/2020, lower stratospheric temperatures were persistently below the threshold for chemical processing earlier than in any other year observed by MLS and remained low approximately as late as in 2011 (Lawrence et al., 2020, describe stratospheric vortex meteorology in 2019/2020).

68 We use MLS version 4 data (Livesey et al., 2020, see supporting information, here-
69 inafter “SI”, for additional details) and meteorological fields from the Modern Era Ret-
70 rospective Analysis for Research and Applications Version 2 (MERRA-2) (Gelaro et al.,
71 2017) to show lower stratospheric polar processing in the extraordinary 2019/2020 win-
72 ter/spring Arctic vortex, resulting record-low ozone, and comparisons with the previous
73 Arctic winters (2010/2011 and 2015/2016) with largest ozone losses.

74 2 Results

75 Figures 1a–g show Northern Hemisphere (NH) MLS maps in December 2010, 2015,
76 and 2019 at 520 K (~ 18 km; approximate level with most polar processing at this time).
77 N_2O within the polar vortex was substantially lower (and H_2O higher) by early Decem-
78 ber 2020 than in either 2015 or 2010, and its gradients across the vortex edge were steeper,
79 consistent with a stronger signature of confined descent and/or descent of lower values
80 from above. By 9 December, the region of temperatures below the nitric acid trihydrate
81 (NAT) polar stratospheric cloud (PSC) threshold (Hanson & Mauersberger, 1988) was
82 larger and more concentric with the vortex in 2019 and 2015 than in 2010. Temperatures
83 remained consistently below this threshold starting earlier in 2019 (by mid-November)
84 than in either 2010 (which did not become cold particularly early) or 2015 (which did)
85 (Lawrence et al., 2020). HNO_3 was depressed in part of the vortex by 9 December in both
86 2019 and 2015, but only 2019 showed substantial chlorine activation; much of the sun-
87 lit portion of the vortex was filled with high ClO by 1 December 2019, with correspond-
88 ingly low HCl values (note that the gridding can make high HCl and high ClO overlap
89 slightly, see SI). Typically, lower stratospheric ozone (O_3) is higher near the vortex edge
90 than in its core before the onset of chemical loss and increases through late December
91 (as in 2015 and 2010). In 2019, however, O_3 was already lower throughout the vortex
92 (even near the inside edge) than outside by 1 December and continued to decline through
93 the month, while it continued increasing outside the vortex as in other years. Along with
94 the early chlorine activation, this suggests very early onset of chemical O_3 loss.

95 Figures 1h–n show 460 K (~ 16 km; approximate level with most ozone loss) maps
96 on dates when extreme values were seen in the polar vortex. By 26 March 2020, N_2O
97 throughout the vortex was even lower compared to other years (and H_2O in regions un-
98 affected by ice PSCs higher) than in December, consistent with an unusually strong con-
99 fined descent signature. In contrast, temperatures remained below the ice PSC thresh-
100 old much longer in 2016 than in any other Arctic winter on record (Manney & Lawrence,
101 2016; Matthias et al., 2016), leading to unprecedented dehydration (Khosrawi et al., 2017).
102 HCl was slightly lower in 2020 than in 2011, which had lower HCl than 2016; consistent
103 with this, ClO was comparably high in 2020 and 2011, and somewhat lower in 2016. MLS
104 recorded no data during 27 March–19 April 2011 because of an instrument anomaly (e.g.
105 Manney et al., 2011). By 26 March, 460 K O_3 was distinctly lower in 2020 than in 2011
106 and remained so through late April, when values started to rise in both years as the vor-
107 tex weakened. Maps of trace gas extrema on MLS retrieval levels (Figs. S1, S2) show con-
108 sistent results, with lower minimum springtime O_3 values in 2020 than in 2011.

109 Figure 2 shows 460 K MLS trace gas evolution comparing 2019/2020 with 2015/2016
110 and 2010/2011 as a function of equivalent latitude (the latitude that would encompass
111 the same area between it and the pole as each potential vorticity, PV, contour, Butchart
112 & Remsberg, 1986) and time, providing a vortex-centered view. In 2019/2020, vortex
113 temperatures (from MERRA-2, Fig. 2a) were comparable to those in 2010/2011 and much
114 lower than climatology in late February through March. Late December through Jan-
115 uary 2015/2016 temperatures are still the lowest on record, with the longest period be-
116 low the ice PSC threshold (e.g., Lawrence et al., 2020); however, since low temperatures
117 are more common during these months than later on, the 2015/2016 temperatures were
118 not as anomalous as those later in the season in 2020 and 2011. Temperatures were anoma-
119 lously low much earlier in the 2019/2020 winter than in 2010/2011.

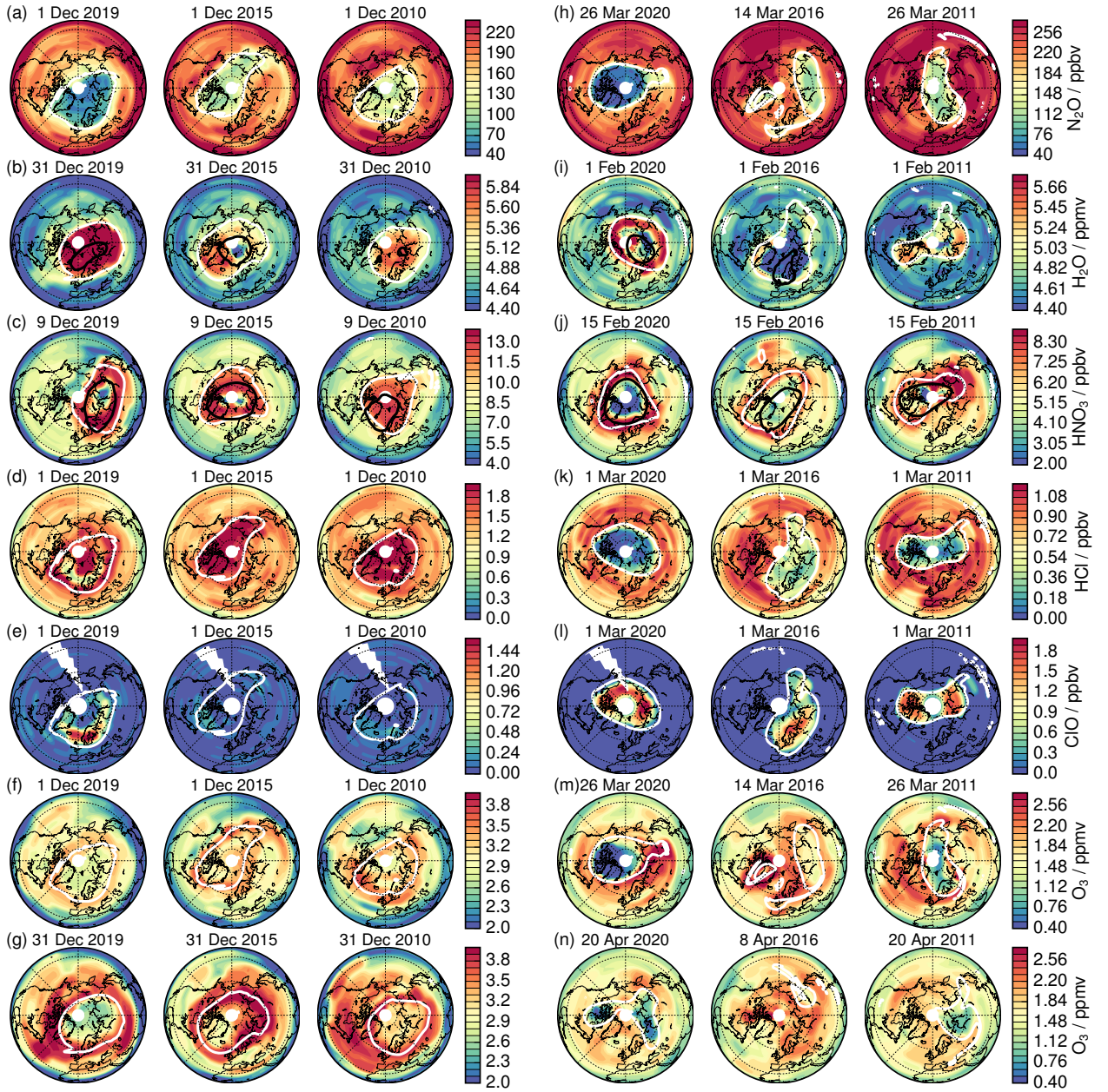


Figure 1. MLS maps: (a–g) 520 K in December and (h–n) 460 K on dates illustrating extreme values, for 2019/2020, 2015/2016, 2010/2011. Overlays: vortex boundary scaled potential vorticity (sPV, white; Lawrence et al., 2018; Lawrence & Manney, 2018); NAT (on HNO_3) and ice (on H_2O) PSC threshold temperatures (black; Lawrence et al., 2018). 26 March (20 April) (m–n for 2011, 2020) is the day before (day after) the 2011 data gap; earlier days are shown for O_3 in 2016 to capture its lowest values before vortex breakup.

120 Vortex strength (Fig. 2a, MERRA-2 overlays) particularly stands out in 2019/2020
121 (see also Lawrence et al., 2020), with PV gradient anomalies in late December 2019 com-
122 parable to those in mid-January 2011 and much stronger PV gradient anomalies as the
123 season progresses than those in 2011 (the previous record-strong lower stratospheric vor-
124 tex, e.g., Manney et al., 2011; Lawrence et al., 2020). The scaled PV (sPV) overlays in
125 Figures 2b-g show that the 2019/2020 vortex also attained its maximum area earlier and
126 maintained it longer than in other years; furthermore, the 2019/2020 vortex was larger
127 than that in 2010/2011 throughout the winter.

128 Figures 2b,c show N_2O and H_2O as the difference from each year's 1 November field
129 to emphasize changes in the confined descent signature through the winter. N_2O decreased
130 more rapidly through February 2020 and developed steeper gradients across the vortex
131 edge, clearly a stronger confined vortex descent signature than in previous years. Before
132 temperatures reached ice PSC thresholds, H_2O also showed this signature, increasing faster
133 in 2019/2020 than in other years. Work in progress indicates that this signature arises
134 largely from a combination of descent of anomalously low N_2O /high H_2O entrained into
135 the developing mid-stratospheric vortex and stronger vortex confinement in 2019/2020
136 than in the other years shown.

137 Consistent with the temperature and vortex evolution, gas-phase HNO_3 remained
138 low longest in 2019/2020: Although negative HNO_3 anomalies were more pronounced
139 in late December/January 2015/2016 and persisted later in 2011, in 2020 low anoma-
140 lies appeared only slightly later than in 2016 and endured as late as in 2011. Moreover,
141 since HNO_3 was anomalously high before the onset of PSCs in 2019/2020, the net de-
142 crease was similar to that in 2016. Significant denitrification occurred in both 2011 and
143 2016 (e.g., Manney et al., 2011; Khosrawi et al., 2017; Johansson et al., 2019), and sim-
144 ilarly low HNO_3 values indicate extensive denitrification in 2020. Several multi-day pe-
145 riods with temperatures below the ice PSC threshold occurred in 2020, notably in late
146 January, and a distinct signature of H_2O sequestration in PSCs is seen in early Febru-
147 ary; this drop (considering higher H_2O values before its onset) is comparable to the ini-
148 tial drop in 2016. Small negative or reduced positive anomalies near the vortex core per-
149 sisted for about a month after temperatures rose above the ice PSC threshold in 2020,
150 suggesting some dehydration; however, 2016 (when low anomalies lingered throughout
151 the season) remains the only Arctic winter in which MLS observed vortex-wide dehy-
152 dration.

153 Chlorine was activated through at least late January in most Arctic winters observed
154 by MLS. HCl (Fig. 2e) dropped to anomalously low values as soon as the vortex was well-
155 defined in 2019/2020 and 2015/2016, whereas chlorine activation in 2010/2011 was near
156 average until late January. ClO values (Fig. 2f) before March depend strongly on vor-
157 tex size and position since much of the vortex may be in darkness; nevertheless, anoma-
158 lously high ClO during December 2019 (compared with near-climatological values un-
159 til late December in the other years) highlights early chlorine activation in 2019/2020.
160 ClO anomalies in March were similarly high in 2020 and 2011. Arctic chlorine deacti-
161 vation normally proceeds though the reformation of ClONO_2 (e.g., Douglass et al., 1995).
162 In all three years highlighted here, however, low- HNO_3 , low-ozone, and low-temperature
163 conditions shifted deactivation towards a more Antarctic-like pathway, with rapid HCl
164 reformation (e.g., Douglass & Kawa, 1999). While we do not know the exact timing of
165 deactivation in 2011 because of the instrument anomaly, the common periods MLS ob-
166 served show similar patterns in 2020 and 2011.

167 The prolonged polar processing in 2019/2020 resulted in substantial low O_3 anoma-
168 lies beginning in early January. Since we expect O_3 to increase via descent in the vor-
169 tex, this pattern suggests appreciable chemical loss beginning by late November 2019.
170 Strong low O_3 anomalies were apparent after early February 2016 and after early March
171 2011. The lowest O_3 observed in 2020 was much lower than that in 2011 at this altitude,
172 and low values covered more area given the larger vortex. Although O_3 may have con-

173 continued to decrease during the data gap in 2011, the area of very low O₃ was never com-
174 parable to that in 2020 (consistent with the extent of lowest values in Fig. 1 and low-
175 est minimum values, Figs. S1 and S2).

176 Vortex averages of MLS data are provided in “Level 3” products that have recently
177 been made public (Livesey et al., 2020, see SI for further description), and cross-sections
178 of them (Fig. 3) show the vertical evolution of vortex trace gases. We focus on 2020 and
179 2011, since the extreme aspects of 2016 (discussed above) did not result in springtime
180 O₃ loss comparable to that in 2020 or 2011. The N₂O and H₂O anomaly fields (and greater
181 convergence in 2020 than in 2011 of the overlaid contours of N₂O values that were at 540
182 and 620 K on 1 November) show strong confined descent. Increased N₂O in April 2020
183 indicates the beginning of the vortex breakup at higher levels (Fig. 3a).

184 The area of potential PSC formation shifted farther downward over the winter in
185 2019/2020 (largest areas near 520–540 K in early winter and 460–480 K by spring) than
186 in 2010/2011 (largest area near ~520 K in early winter and ~500 K by spring). Low HNO₃
187 anomalies follow this vertical progression. In 2019/2020, increasing high HNO₃ anoma-
188 lies in late December and January below the cold region suggest renitrification through
189 evaporation of PSCs sedimenting from above; similar, albeit smaller, anomalies were seen
190 in January 2011. High H₂O anomalies during most of 2019/2020, consistent with the strong
191 confined descent signature in N₂O, are related to initially low/high mid-stratospheric N₂O/H₂O;
192 the abrupt shift from strong high anomalies to no significant anomalies in late January
193 to early February 2020 reflects a period with substantial ice PSC activity. H₂O anoma-
194 lies were weak in 2011 as ice PSCs were infrequent.

195 Chlorine activation as seen in HCl and ClO (Figs. 3d,e) is consistent with the ev-
196 idence of PSC activity in temperatures and HNO₃: The region with greatest HCl deple-
197 tion was at lower altitudes in winter/spring 2019/2020 than in 2010/2011 (spring min-
198 imum HCl values near ~480 K in 2020 versus ~520 K in 2011). Maximum ClO values
199 were near 460 K throughout March 2020 and moved from ~520 K to ~480 K from early
200 to late March in 2011. Anomalously high ClO in December 2019 and early January 2020
201 was consistent with HCl, but varied depending on how much of the vortex experienced
202 sunlight; in contrast, HCl in December 2010 was slightly higher than climatology, indi-
203 cating a relatively late start to chlorine activation.

204 Ozone contours (Fig. 3f) tilt downward through November, consistent with the strong
205 descent signature seen in N₂O and H₂O. Since strong descent was ongoing through De-
206 cember, the flattening of O₃ contours and appearance of negative O₃ anomalies suggest
207 that chemical O₃ loss began by late November and overwhelmed replenishment by de-
208 scent by early December 2019. In 2011, strong negative O₃ anomalies first appeared in
209 February. Although the 2011 MLS record is incomplete, no evidence suggests that O₃
210 reached values as low as those in 2020. Further, minimum vortex-averaged O₃ occurred
211 near 440–460 K in 2020 but 480–500 K in 2011; thus even when values dipped as low in
212 2011, they were at smaller pressures and consequently affected the total column less. Record-
213 low column ozone and associated record-high surface ultraviolet will be discussed in other
214 papers in this special collection (e.g., Bernhard et al., 2020; Grooß & Müller, 2020; Wohlt-
215 mann et al., 2020).

216 Vortex-averaged profiles on individual days (Fig. 3, right column) quantify differ-
217 ences between 2020 and 2011. Confined descent was stronger and PSC activity greater
218 in 2020 than in 2011. Chlorine activation was similar at lower altitudes in both years but
219 stronger at higher altitudes in 2011. O₃ abundances were smaller below ~500 K in 2020
220 than in 2011. Fig. S3 shows raw MLS profiles indicating that, though vortex averages
221 were only slightly lower in 2020 than in 2011, localized minimum values were near zero
222 in late March 2020, compared to ~0.5 ppmv in 2011, and occurred at lower altitude. Com-
223 parisons of time series of minima from ozonesondes and MLS data (Wohltmann et al.,
224 2020) show consistent results.

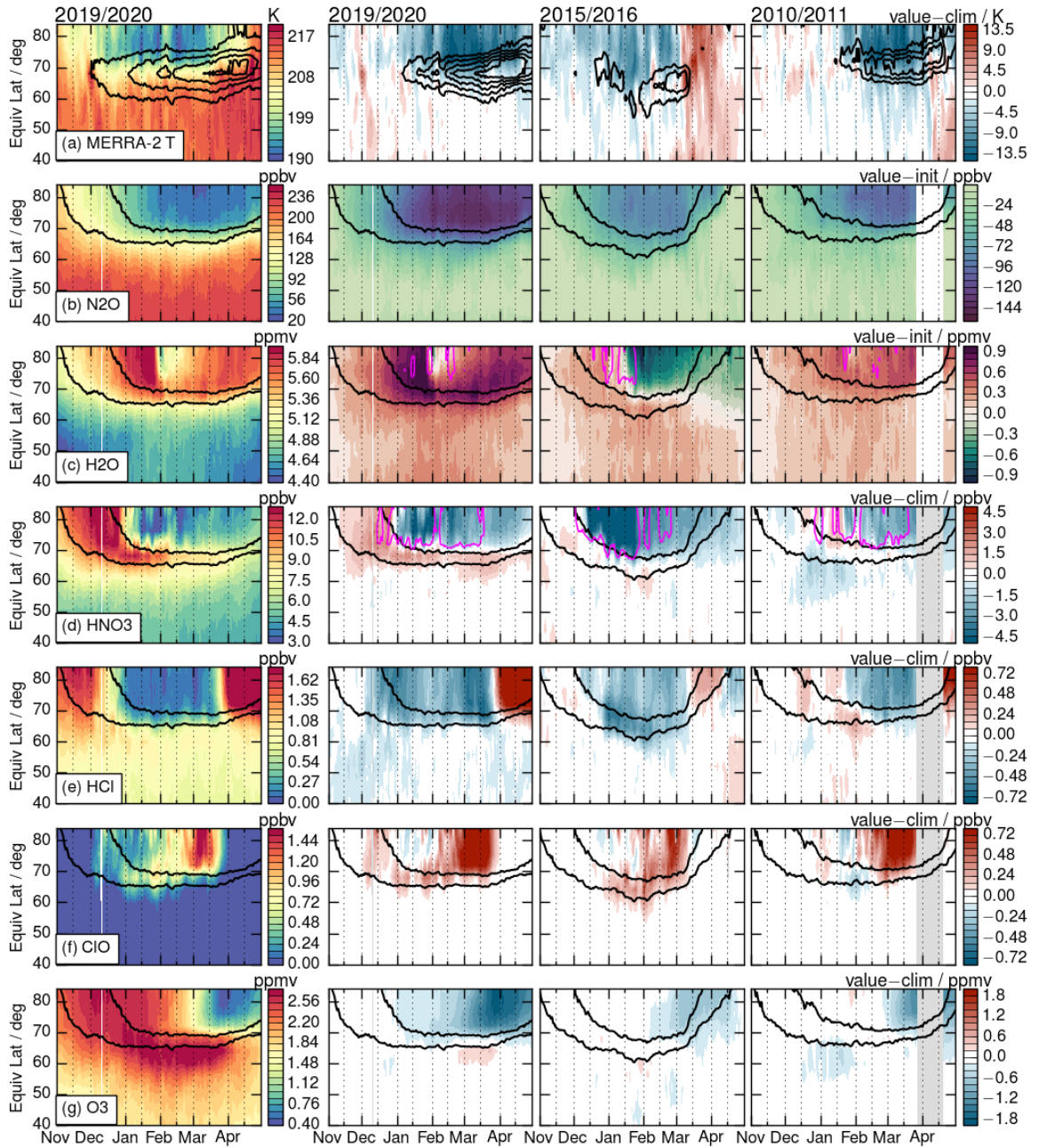


Figure 2. (a) 460 K EqL/time plots of MERRA-2 temperature for 2019/2020 (left), and difference from 2004/2005–2019/2020 climatology for (following columns) 2019/2020, 2015/2016, and 2010/2011; overlays: (left) sPV gradients with respect to EqL, and (remaining columns) sPV gradient differences from climatology (positive values only, showing where sPV gradients are stronger than climatology). (b–c) EqL/time plots of 460 K MLS N_2O and H_2O for 2019/2020 (left), and differences from the 1 November values (remaining columns). (d–g) As in (b–c), but for other MLS trace gases and differences from climatology; overlays: sPV in vortex edge region (black, $1.4, 1.8 \times 10^{-4} \text{s}^{-1}$), temperature (magenta; 197 K on HNO_3 , 192 K on H_2O ; values higher than the PSC thresholds, for NAT and ice, respectively, are shown to approximate the region where some values around the EqL contour are below those thresholds).

225 Figure 3g shows estimates of chemical O₃ loss using the “MLS Match” method (Livesey
226 et al., 2015, also see SI). The computed cumulative chemical change in 2019/2020 indi-
227 cates some early chemical loss above 520 K, but largest loss between about 400 and 470 K.
228 Similar loss rates were computed for 2020 and 2011 through late March, with maximum
229 losses near 2.8 ppmv. However, consistent with observed chlorine activation, maximum
230 losses were at lower altitude in 2020 than in 2011.

231 3 Summary and Conclusions

232 Figure 4 summarizes chemical processing and ozone loss at 460 and 520 K in 2019/2020
233 in comparison to the other winters observed by Aura MLS. Descent of unusually low N₂O
234 from the mid-stratosphere together with a well-isolated vortex resulted in smaller N₂O
235 abundances in the lower stratosphere in 2020 than in any previous winter observed by
236 MLS. Depressed gas-phase HNO₃ shows the onset of sequestration in PSCs in Decem-
237 ber; although the timing varied with altitude, the magnitude of the decrease was larger
238 in 2019/2020. An abrupt drop in H₂O in late January 2020 indicates sequestration in
239 ice PSCs, but temperatures rose above the ice PSC threshold again too soon to produce
240 vortex-wide dehydration of similar magnitude to that in 2016. Although H₂O decreased
241 over a small altitude range in 2020, at 460 K the drop during the coldest period was com-
242 parable to that in 2016 (and, when the altitude range is considered, larger than that in
243 2010 reported by, e.g., Khaykin et al., 2013).

244 Chlorine activation began slightly earlier in 2019 than in 2015 at 460 K and ear-
245 lier than in 2010 at all levels. Previously, earliest strong Arctic chlorine activation was
246 observed in 2012/2013, and the vortex was sufficiently exposed to sunlight for ClO to
247 be elevated in late December (Manney et al., 2015). The timing of the HCl drop in 2019
248 was similar to that in 2012 at 460 K, but about ten days earlier at 520 K; at both lev-
249 els highly elevated ClO was seen nearly two weeks earlier in 2019 than in 2012.

250 In 2011, chlorine deactivation occurred much later and followed a more Antarctic-
251 like pattern than previously observed in the Arctic (e.g., Manney et al., 2011). The tim-
252 ing and pathway of chlorine deactivation in 2020 approximated Antarctic patterns even
253 more closely. Not only did ClO remain enhanced at 460 K as late as in 2011, but also
254 HCl recovered much faster than usual and reached considerably higher values by mid-
255 April than in 2011. In a typical Arctic spring, deactivation initially proceeds through
256 reformation of ClONO₂; however, several factors can shift Arctic chlorine partitioning
257 toward HCl as in the Antarctic (e.g., Douglass et al., 1995; Santee et al., 2008). First,
258 denitrification limits the availability of NO₂, inhibiting combination with ClO to form
259 ClONO₂. In addition, low ozone and low temperatures together lead to preferential ref-
260 ormation of HCl (e.g., Douglass & Kawa, 1999). Thus HCl production was highly favored
261 inside the persistently cold, strongly denitrified, and ozone-depleted Arctic vortex in spring
262 2020. Atmospheric Chemistry Experiment-Fourier Transform Spectrometer ClONO₂ data
263 (Boone et al., 2013) (Fig. S6, Text S4) and model results (Groß & Müller, 2020) are
264 consistent with this picture.

265 These conditions resulted in record-low Arctic O₃ values in spring 2020 at levels
266 below ~500 K, and record low MLS stratospheric column values (see SI). Match estimates
267 suggest more chemical loss in December 2019 through April 2020 than in 2010/2011 be-
268 low ~460 K; peak losses were near 2.8 ppmv in each of these winters, but at lower alti-
269 tude in 2020 than in 2011. While empirical O₃ loss estimates have large uncertainties
270 (e.g., Griffin et al., 2019, also see SI), vortex-averaged descent calculations using MLS
271 N₂O (overlaid lines/symbols in Fig. 4f,l) and using trajectory-based descent rates (over-
272 laid symbols in Fig. 4) (see SI for description of calculations) give consistent results; Groß
273 and Müller (2020) and Wohltmann et al. (2020) report similar results using different datasets
274 and methods. We find that chemical loss between December and March was very sim-
275 ilar in the two winters, but significant chemical loss occurred in November only in 2019.

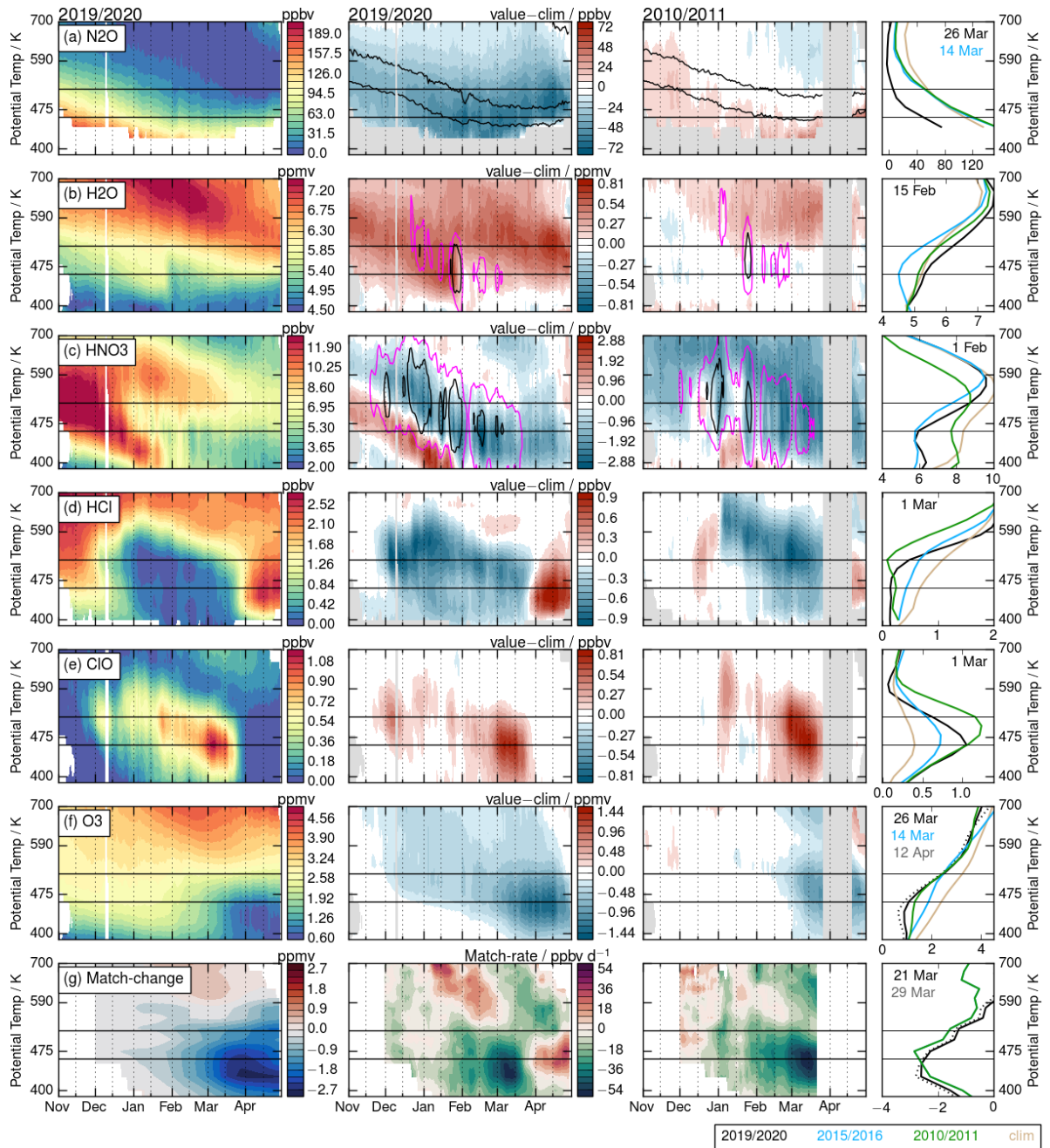


Figure 3. (a–f) Potential temperature/time sections of (left) 2019/2020 vortex-averaged (see SI) MLS species, and (center columns) differences from 2004/2005–2019/2020 climatology for 2019/2020 and 2010/2011; right column: 2011, 2016, and 2020 profiles on extreme dates, and climatology (for 2020 dates where those differ from other years). Black overlays in (a) show contours of N_2O values that were at 540 and 620 K on 1 November. Overlays in (b) show area with MERRA-2 temperatures below the ice PSC threshold (magenta shows 1% and black 2% of NH) and in (c) below the NAT threshold (magenta shows 3% and black 5% of NH). (g) (left) Cumulative chemical O_3 change in 2020 from Match (see text and SI), (center columns) Match rate of O_3 change in 2020 and 2011, and (right) cumulative O_3 change profiles on 21 March 2020 and 2011, and 29 March 2020 (dotted line). Horizontal lines mark 520 and 460 K. X-axis units for profiles are the same as left column of corresponding row.

(As explained in the SI, the vortex-averaged descent methods give slightly lower estimates than Match because they may be more affected by dilution of the chemical loss signature near the vortex edge.) Record-low springtime O₃ at lower altitudes in 2020 than in 2011 is consistent with evidence of record-low total column O₃ (Grooß & Müller, 2020; Wohltmann et al., 2020) and anomalously high surface ultraviolet in 2020 (Bernhard et al., 2020). Large interannual variability in meteorological conditions in the Arctic stratosphere (which led to the exceptionally strong and long-lived polar vortex in 2019/2020) may yet result in more extreme Arctic O₃ loss in future years while stratospheric chlorine loading remains high: For instance, 2015/2016 still stands out as the coldest Arctic winter with most denitrification and dehydration – if conditions such as those commenced as early in some future year and lasted as late as in 2019/2020, and the vortex remained well-isolated, then greater O₃ depletion could occur. This variability, coupled with likely effects of climate change, makes comprehensive monitoring of polar processes such as that provided by Aura MLS (currently in the 16th year of a 5-year mission) an important priority moving forward.

Acknowledgments

We thank the Microwave Limb Sounder team at JPL, especially Brian Knosp, for MLS retrieval processing, and computational, data processing, management, and analysis support; NASA’s GMAO for providing their assimilated data products; and Germar Bernhard, Vitali Fioletov, Jen-Uwe Grooß, Rolf Müller, and Ingo Wohltmann for helpful discussions, and two anonymous reviewers for their careful and valuable comments. GLM and ZDL were partially supported by the JPL Microwave Limb Sounder team under JPL subcontracts to NWRA. Work at the Jet Propulsion Laboratory, California Institute of Technology was done under contract with the National Aeronautics and Space Administration. The datasets used here are publicly available:

- MERRA-2: <https://disc.sci.gsfc.nasa.gov/uui/datasets?keywords=%22MERRA-2%22>
- Aura MLS Level-2 and Level-3 data: <https://disc.gsfc.nasa.gov/datasets?page=1&keywords=AURA%20MLS>
- ACE-FTS v3.6 data: <http://www.ace.uwaterloo.ca> (registration required)

References

- Bernhard, G. H., Fioletov, V. E., Grooß, J.-U., Ialongo, I., Johnsen, B., Lakkala, K., . . . Svenby, T. (2020). *Record-breaking increases in Arctic solar ultraviolet radiation caused by exceptionally large ozone depletion in 2020*. (to be submitted to GRL for this special collection)
- Boone, C. D., Walker, K. A., & Bernath, P. F. (2013). Version 3 retrievals for the Atmospheric Chemistry Experiment Fourier Transform Spectrometer (ACE-FTS). In P. F. Bernath (Ed.), *The Atmospheric Chemistry Experiment ACE at 10: A solar occultation anthology* (pp. 103–127). A. Deepak Publishing.
- Butchart, N., & Remsberg, E. E. (1986). The area of the stratospheric polar vortex as a diagnostic for tracer transport on an isentropic surface. *J. Atmos. Sci.*, *43*, 1319–1339.
- Douglass, A. R., & Kawa, S. R. (1999). Contrast between 1992 and 1997 high-latitude spring Halogen Occultation Experiment observations of lower stratospheric HCl. *J. Geophys. Res.*, *104*(D15), 18,739–18,754.
- Douglass, A. R., Schoeberl, M. R., Stolarski, R. S., Waters, J. W., III, J. M. R., Roche, A. E., & Massie, S. T. (1995). Interhemispheric differences in spring-time production of HCl and ClONO₂ in the polar vortices. *J. Geophys. Res.*, *100*, 13,967–13,978.
- Gelaro, R., McCarty, W., Suarez, M. J., Todling, R., Molod, A., Takacs, L., . . .

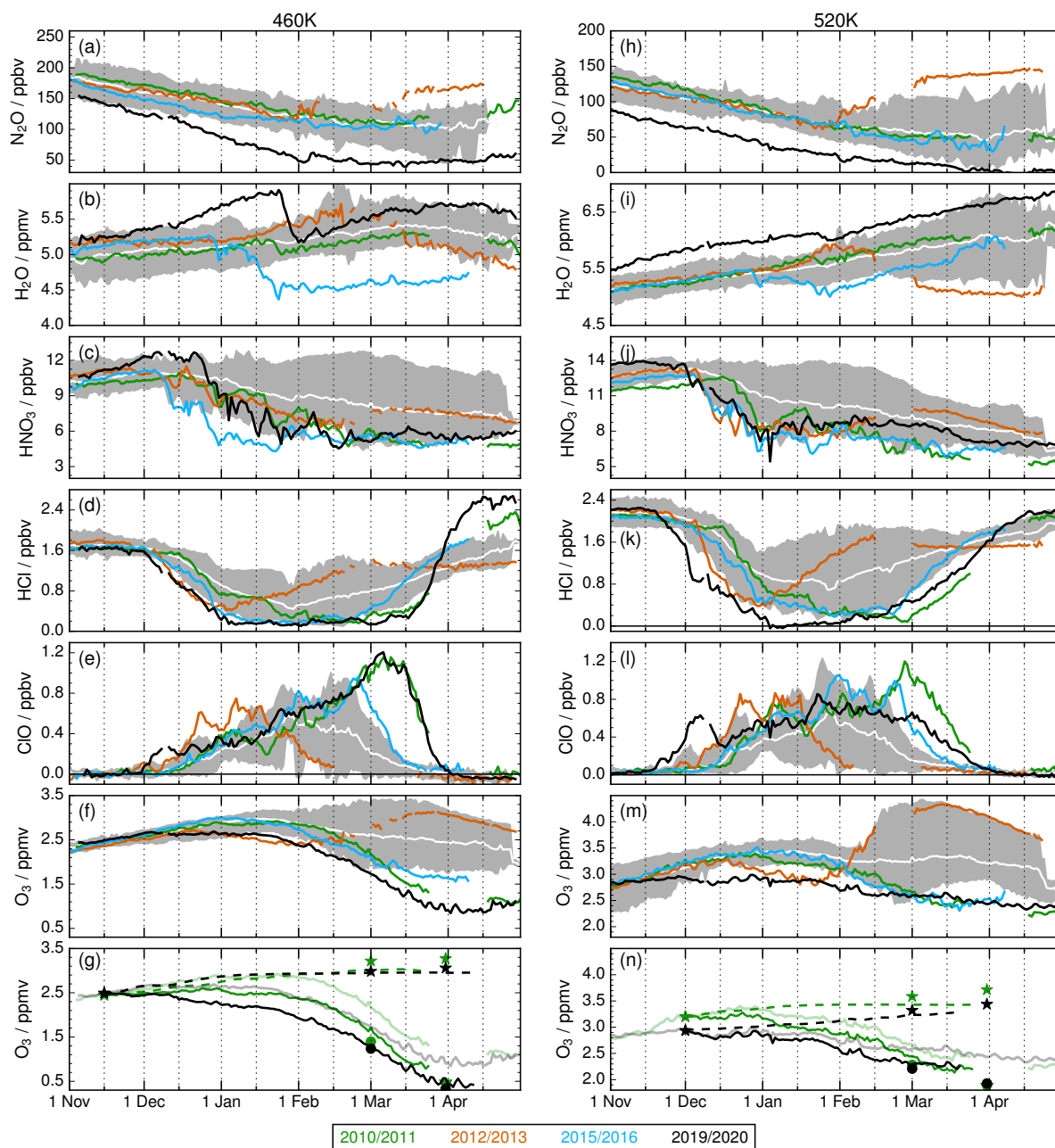


Figure 4. Vortex-averaged MLS trace gases for 2019/2020 (black), 2015/2016 (blue), 2012/2013 (orange), and 2010/2011 (green), at (a–g) 460 K and (h–n) 520 K. Grey envelope shows range of values for 2004/2005 through 2018/2019, excluding the highlighted years; white line shows mean for those years. (g) and (n) show passive ozone (dashed lines) and calculated chemical ozone loss (solid lines) estimated from MLS N_2O gradients (see SI) for 2011 (green) and 2020 (black), with observed evolution in pale colors; overlaid symbols show initial and passive ozone (stars) and trajectory-based chemical loss estimates (circles) (see SI); green triangles on 31 March (partially obscured by black circles) show 2011 chemical loss estimated using the average of two days bordering the data gap for the observed value.

- 326 Zhao, B. (2017). The Modern-Era Retrospective Analysis for Research
327 and Applications, Version-2 (MERRA-2). *J. Clim.*, *30*, 5419–5454. doi:
328 doi:10.1175/JCLI-D-16-0758.1
- 329 Griffin, D., Walker, K. A., Wohltmann, I., Dhomse, S. S., Rex, M., Chipperfield,
330 M. P., . . . Tarasick, D. (2019). Stratospheric ozone loss in the Arctic winters
331 between 2005 and 2013 derived with ACE-FTS measurements. *Atmos. Chem.*
332 *Phys.*, *19*(1), 577–601. Retrieved from [https://www.atmos-chem-phys.net/
333 19/577/2019/](https://www.atmos-chem-phys.net/19/577/2019/) doi: 10.5194/acp-19-577-2019
- 334 Grooß, J.-U., & Müller, R. (2020). *Simulation of the record Arctic stratospheric*
335 *ozone depletion in 2020*. (Submitted to *J. Geophys. Res.*)
- 336 Hanson, D., & Mauersberger, K. (1988). Laboratory studies of the nitric acid trihy-
337 drate: Implications for the south polar stratosphere. *Geophys. Res. Lett.*, *15*,
338 855–858.
- 339 Johansson, S., Santee, M. L., Grooß, J.-U., Höpfner, M., Braun, M., Friedl-
340 Vallon, F., . . . Woiwode, W. (2019). Unusual chlorine partitioning in the
341 2015/16 Arctic winter lowermost stratosphere: observations and simula-
342 tions. *Atmos. Chem. Phys.*, *19*(12), 8311–8338. Retrieved from [https://
343 www.atmos-chem-phys.net/19/8311/2019/](https://www.atmos-chem-phys.net/19/8311/2019/) doi: 10.5194/acp-19-8311-2019
- 344 Khaykin, S. M., Engel, I., Vömel, H., Formanyuk, I. M., Kivi, R., Korshunov, L. I.,
345 . . . Peter, T. (2013). Arctic stratospheric dehydration. Part 1: Unprece-
346 dented observation of vertical redistribution of water. *Atmos. Chem. Phys.*,
347 *13*, 11,503–11,517.
- 348 Khosrawi, F., Kirner, O., Sinnhuber, B.-M., Johansson, S., Höpfner, M., Santee,
349 M. L., . . . Braesicke, P. (2017). Denitrification, dehydration and ozone loss
350 during the 2015/2016 Arctic winter. *Atmos. Chem. Phys.*, *17*(21), 12893–
351 12910. Retrieved from [https://www.atmos-chem-phys.net/17/12893/2017/
352 doi: 10.5194/acp-17-12893-2017](https://www.atmos-chem-phys.net/17/12893/2017/)
- 353 Kuttippurath, J., Godin-Beekmann, S., Lefèvre, F., Nikulin, G., Santee, M. L.,
354 & Froidevaux, L. (2012). Record-breaking ozone loss in the Arctic winter
355 2010/2011: comparison with 1996/1997. *Atmos. Chem. Phys.*, *12*, 7073–7085.
- 356 Lawrence, Z. D., & Manney, G. L. (2018). Characterizing stratospheric polar
357 vortex variability with computer vision techniques. *Journal of Geophysical Re-*
358 *search: Atmospheres*, *123*(3), 1510–1535. Retrieved from [http://dx.doi.org/
359 10.1002/2017JD027556](http://dx.doi.org/10.1002/2017JD027556) (2017JD027556) doi: 10.1002/2017JD027556
- 360 Lawrence, Z. D., Manney, G. L., & Wargan, K. (2018). Reanalysis intercomparisons
361 of stratospheric polar processing diagnostics. *Atmos. Chem. Phys.*, *18*, 13547–
362 13579. doi: 10.5194/acp-18-13547-2018
- 363 Lawrence, Z. D., et al. (2020). *The remarkably strong Arctic stratospheric polar vor-*
364 *tex of winter 2020: Ties to record-breaking Arctic oscillation and ozone loss*.
365 (to be submitted to *JGR* for this special collection)
- 366 Livesey, N. J., Read, W. G., Wagner, P. A., Froidevaux, L., Lambert, A., Man-
367 ney, G. L., . . . Lay, R. R. (2020). *EOS MLS version 4.2x level 2 and 3*
368 *data quality and description document* (Tech. Rep.). JPL. (Available from
369 <http://mls.jpl.nasa.gov/>)
- 370 Livesey, N. J., Santee, M. L., & Manney, G. L. (2015). A Match-based approach to
371 the estimation of polar stratospheric ozone loss using Aura Microwave Limb
372 Sounder observations. *Atmos. Chem. Phys.*, *15*, 9945–9963.
- 373 Manney, G. L., & Lawrence, Z. D. (2016). The major stratospheric final warming in
374 2016: dispersal of vortex air and termination of Arctic chemical ozone loss. *At-*
375 *mos. Chem. Phys.*, *16*(23), 15371–15396. Retrieved from [https://www.atmos
376 -chem-phys.net/16/15371/2016/](https://www.atmos-chem-phys.net/16/15371/2016/) doi: 10.5194/acp-16-15371-2016
- 377 Manney, G. L., Lawrence, Z. D., Santee, M. L., Livesey, N. J., Lambert, A., & Pitts,
378 M. C. (2015). Polar processing in a split vortex: Arctic ozone loss in early
379 winter 2012/2013. *Atmos. Chem. Phys.*, *15*, 4973–5029.
- 380 Manney, G. L., Santee, M. L., Rex, M., Livesey, N. J., Pitts, M. C., Veefkind, P., . . .

- 381 Zinoviev, N. S. (2011). Unprecedented Arctic ozone loss in 2011. *Nature*, *478*,
 382 469–475.
- 383 Matthias, V., Drnbrack, A., & Stober, G. (2016). The extraordinarily strong and
 384 cold polar vortex in the early northern winter 2015/2016. *Geophys. Res.*
 385 *Lett.*, *43*(23), 12,287–12,294. Retrieved from [http://dx.doi.org/10.1002/](http://dx.doi.org/10.1002/2016GL071676)
 386 [2016GL071676](http://dx.doi.org/10.1002/2016GL071676) (2016GL071676) doi: 10.1002/2016GL071676
- 387 Santee, M. L., MacKenzie, I. A., Manney, G. L., Chipperfield, M. P., Bernath, P. F.,
 388 Walker, K. A., ... Waters, J. W. (2008). A study of stratospheric chlorine
 389 partitioning based on new satellite measurements and modeling. *J. Geophys.*
 390 *Res.*, *113*. doi: 10.1029/2007JD009057
- 391 Sinnhuber, B.-M., Stiller, G., Ruhnke, R., von Clarmann, T., Kellmann, S., & As-
 392 chmann, J. (2011). Arctic winter 2010/2011 at the brink of an ozone hole.
 393 *Geophys. Res. Lett.* doi: 10.1029/2011GL049784
- 394 WMO. (2014). *Scientific assessment of ozone depletion: 2014*. Geneva, Switzerland:
 395 Global Ozone Res. and Monit. Proj. Rep. 55.
- 396 WMO. (2018). *Scientific assessment of ozone depletion: 2018*. Geneva, Switzerland:
 397 Global Ozone Res. and Monit. Proj. Rep. 55.
- 398 Wohltmann, I., von der Gathen, P., Lehmann, R., Maturilli, M., Deckelmann, H.,
 399 Manney, G. L., ... Rex, M. (2020). *Near complete local reduction of Arctic*
 400 *stratospheric ozone by severe chemical loss in spring 2020*. (Submitted to
 401 *Geophys. Res. Lett.*)